NATIONAL ADVISORY COMMITTEE FOR AERONAUTICS

TECHNICAL NOTE 3544

COMPARISON BETWEEN THEORETICAL AND EXPERIMENTAL STRESSES IN CIRCULAR SEMIMONOCOQUE CYLINDERS WITH RECTANGULAR CUTOUTS

By Harvey G. McComb, Jr., and Emmet F. Low, Jr.

Langley Aeronautical Laboratory
Langley Field, Va.

Washington
October 1955

NATIONAL ADVISORY COMMITTEE FOR AERONAUTICS

TECHNICAL NOTE 3544

COMPARISON BETWEEN THEORETICAL AND EXPERIMENTAL STRESSES IN CIRCULAR SEMIMONOCOQUE CYLINDERS WITH RECTANGULAR CUTOUTS

By Harvey G. McComb, Jr., and Emmet F. Low, Jr.

SUMMARY

Comparisons are made between a theory for calculating stresses about rectangular cutouts in circular cylinders of semimonocoque construction published in NACA TN 3200 and previously published experimental data. The comparisons include stresses in the stringers and shear stresses in the center of the shear panels in the neighborhood of the cutout. The theory takes into account the bending flexibility of the rings in the structure, and this factor is found to be important in the calculation of stresses about cutouts. In general, when the ring flexibility is considered, good agreement is obtained between the calculated and experimental results.

INTRODUCTION

In the design of airplane fuselages near cutouts, such as those made for doors and windows, it is desirable to have some knowledge of the redistribution of stress which is introduced into the structure by the opening. A large portion of the structure of many fuselages can be represented, approximately, by a circular cylinder of semimonocoque construction, that is, a thin-walled circular cylinder stiffened by stringers (axial stiffening members) and rings (circumferential stiffening members). A method for calculating stresses about rectangular cutouts in such structures is presented in reference 1. In order to evaluate this method, comparisons are made between stringer stresses and shear stresses in the vicinity of the cutout as calculated by the theory of reference 1 and those obtained by experiment in references 2 to 4. These comparisons are presented herein. The experimental data were obtained from a single test cylinder under several loading conditions and with successively larger cutout sizes. All the loading conditions and four of the cutout sizes reported in references 2 to 4 are considered. The effect of the bending flexibility of the rings in their own planes is

taken into account. In order to determine the importance of this effect in the calculation of stresses about cutouts, the results of calculations based on the assumption that the rings are rigid in their own planes are also presented.

SYMBOLS

A effective cross-sectional area of stringer, sq in.

$B = \frac{E}{G} \frac{A}{bt} \frac{R^2}{L^2}$

b arc distance between stringers, in.

$C = \frac{AR^6}{IL^3b}$

E Young's modulus of elasticity, ksi

G shear modulus of elasticity, ksi

I effective moment of inertia of ring cross section, $in.^4$

L distance between rings, in.

M moment, kip-in.

m total number of stringers in cylinder

R radius of cylinder (measured to middle surface of sheet), in.

T torque, kip-in.

t thickness of sheet, in.

V shear force, kip

β circumferential length of cutout, deg

θ circumferential distance around cylinder measured from center line of cutout, deg

TESTS

A detailed description of the experimental program can be found in references 2 to 4; therefore, only a brief description of the test cylinder and test setup will be given here. The test cylinder is illustrated in figure 1. It was constructed of 2024 (formerly 24S) aluminum alloy and consisted of a thin-walled circular cylinder reinforced by 36 stringers and 8 rings. The stringers were extruded angles and the rings were Z-sections formed from sheet material. The rings were stiffer than would normally be used in the present-day design of a fuselage for a large transport.

The cylinder was cantilevered from a large backstop by mounting one end on a steel ring which was bolted to the backstop. A steel bulkhead was fitted to the free end, and torque, bending, and shear external loads were applied to this free end with a hydraulic jack acting through appropriate loading frames.

A single rectangular cutout was made in the center bay of the cylinder. The original cutout extended 30° around the circumference. During the test program, this cutout was successively enlarged in the circumferential direction to 50°, 70°, 90°, and 130°. Finally, the 130° cutout was extended 1 bay toward the free end of the cylinder so that the cutout was 2 bays long. Electrical resistance wire strain gages were used to measure strains around the cutout, and stresses were calculated by use of the material moduli.

CALCULATIONS

Parameters

The application of the method of analysis of reference 1 is facilitated by the use of the tables of coefficients published in reference 5. In order to determine the appropriate table of reference 5 to be used in the calculations, the values of two structural parameters $B = \frac{E}{G}\frac{A}{bt}\frac{R^2}{L^2}$ and $C = \frac{AR^6}{\pi L^3 b}$ are computed. The properties of the test cylinder (fig. 1) are as follows:

m	36
Cross-sectional area of stringer, sq in.	0.1373
R, in.	15
L, in.	12

t, in.	0.051
b, in.	2.62
Moment of inertia of ring cross section, $in.^4$	0.275
E, ksi	10.6×10^3
G, ksi	4×10^3

The entire skin is assumed to be effective in carrying direct stresses; therefore, the effective stringer area is

$$A = 0.1373 + (2.62)(0.051) = 0.271 \text{ sq in.}$$

Consequently,

$$B = \frac{10.6 \times 10^3 \times 0.271}{4 \times 10^3 \times 0.134}\left(\frac{15}{12}\right)^2 = 8.37$$

The parameter C involves the effective moment of inertia of a ring cross section; therefore, some estimate is needed of the amount of skin which acts with a ring in bending. Investigations of this problem are reported in references 6 and 7. From reference 6 it is found that in the test cylinder the rings are sufficiently far apart so that for each ring the effective width of skin is practically the same as the effective width acting with a single ring mounted on an infinitely long circular cylindrical shell. In reference 7 this effective width of skin which acts with a ring on an infinitely long circular cylinder is given as approximately $1.52\sqrt{Rt}$, provided the skin thickness is small with respect to the cylinder radius and provided the loading on the ring does not oscillate rapidly in the circumferential direction. For the test specimen this effective width is

$$1.52\sqrt{(15)(0.051)} = 1.33 \text{ inches}$$

The effective moment of inertia of a ring when 1.33 inches of skin is acting with it in bending is 0.346 $inch^4$. Consequently,

$$C = \frac{(0.271)(15)^6}{(0.346)(12)^3(2.62)} = 1{,}970$$

The table of reference 5 which corresponds most closely to the test specimen (table 11 of ref. 5 for which $B = 8$ and $C = 2{,}000$) was used to make the calculations for this report. No significant change in the results would occur if the calculations were made by interpolating between tables.

It is common practice in the analysis of a fuselage to neglect the distortions of the rings in their own planes. In order to assess the importance of taking into account the flexibility of the rings, further calculations were made based on the assumption that the rings are rigid in their own planes (by utilizing table 1 of ref. 5 where $B = 8$, $C = 0$). Thus, a comparison between rigid-ring and flexible-ring theory is included.

Coaming Stringer Stresses

The effective area of the coaming stringers changes abruptly at the corners of the cutout in the test specimen. In the net section the portion of effective skin on the cutout side of the coaming stringer has been removed. This discontinuity can be taken into account by assuming that in the net section the coaming stringer has a reinforcement of negative area equal to the portion of effective skin removed and then applying the procedure described in reference 1 for analyzing a structure which has stringer reinforcement. A simpler but more approximate procedure, however, is to compute stringer loads without considering the reduction in coaming-stringer area and then take this effect into account when the stringer stresses are computed. The latter procedure was utilized in the calculations for this report.

The effective skin for the coaming stringers in the net section was taken as the area of skin from the cutout side of the coaming stringer to the line halfway between the rivet lines of the coaming stringer and its adjacent uninterrupted stringer. The effective coaming stringer area in the net section is

$$0.1373 + (1.74)(0.051) = 0.226 \text{ sq in.}$$

The stringer loads were calculated on the basis of an effective stringer area of 0.271 sq in. Then, in order to calculate the stress in the portion of coaming stringer in the net section of the cylinder, the effective area of 0.226 sq in. was used. In order to calculate the stress in the coaming stringer in the gross section and the stresses in the remaining stringers, the effective area of 0.271 sq in. was used.

COMPARISONS

Comparisons between experimental and theoretical stresses in the test cylinder are shown in figures 2 to 9 for four loading conditions: pure torsion, pure bending with cutout on tension side, shear with cutout on tension side, and shear with cutout centered on neutral axis. Comparisons are presented for four sizes of cutout: 1 bay in length by

50° in circumference, 1 bay by 90°, 1 bay by 130°, and 2 bays by 130°. The theoretical stresses shown in figures 2 to 9 include the results of flexible-ring and rigid-ring analyses as well as calculations in which the cutout is disregarded and elementary bending and torsion theories are used.

In the theory of reference 1 the shear stress is assumed to be constant within each shear panel and the calculated shear stress in a given panel should be considered as the average shear stress for that panel. On the other hand, the test results of references 2 to 4 indicate that, in many cases, an appreciable variation of shear stress occurs within a panel. A fair comparison would be between calculated shear stresses and average experimental shear stresses. There is, however, insufficient test data to obtain a satisfactory estimate of the average shear stress in many panels where comparisons should be made. In the comparisons which follow, the experimental shear stresses plotted are those obtained from the gages in the center of the panels because this procedure affords the advantages of simplicity and consistency in an instance where a more complicated procedure would not necessarily yield a more accurate value for the average shear stress. These experimental shear stresses will be called "center shear stresses."

The location on the cylinder of the stresses which are plotted in figures 2 to 9 varies somewhat from one case to another in order that the plotted stresses will always include the highest stringer stresses and the highest center shear stresses in the vicinity of the cutout.

The theory of reference 1 does not strictly apply when the cutout is more than one bay long because the effect of interrupting a ring cannot be taken into consideration in the theory without the introduction of additional types of perturbation loads. The theoretical stresses, which are plotted for the 130° two-bay cutouts, were calculated by using the same properties of the cylinder as were used for the one-bay cutouts and by ignoring the effects of interrupting the ring at the center line of the cutout.

Torsion

Shear stresses and stringer stresses for a cylinder in pure torsion are shown in figures 2 and 3, respectively. For the one-bay cutouts, the experimental shear stresses are obtained from gages mounted at the center line of the cutout on successive shear panels in the circumferential direction. For the 130° two-bay cutout, the experimental shear stresses are obtained from gages mounted on the center line of one of the cut bays rather than on the center line of the cutout.

For the one-bay cutouts the largest error in predicting the maximum center shear stress occurs for $\beta = 130°$ (fig. 2(c)) where the theoretical value is 7 percent low. In the case of the 130° two-bay cutout

(fig. 2(d)), the highest center shear stress in one of the cut bays as predicted by the theory was 14 percent low. At the coaming ring the experimental maximum coaming-stringer stresses fall between the calculated maximum net and gross section stresses in every case except for the 130° two-bay cutout (fig. 3(d)) where the test result lies 5 percent above the calculated net section stress.

Pure Bending With Cutout on Tension Side

The stresses shown in figures 4 and 5 are for a cylinder under pure bending with the cutout located on the tension side. The shear stresses that are plotted in figure 4 occur in the bay adjacent to the cutout. The experimental shear stresses are obtained from gages located in the center of the shear panels as before. The calculated shear stresses agree very well with the experimental center shear stresses except in the panels which are adjacent to the coaming stringer and in which the highest shear stresses occur. In these panels the agreement is good for the 50° cutout (fig. 4(a)) but becomes poorer as the cutout size increases; and, for the 130° one-bay cutout (fig. 4(c)), the theoretical stress is 30 percent high. An examination of the test results in reference 3 indicates that the comparison probably would be better in these shear panels if the true average shear stress were plotted rather than the center shear stress. In the case of the 130° two-bay cutout (fig. 4(d)), there were no gages located in the center of the shear panels having the highest shear stress.

The stringer stresses shown in figure 5 are those at the center line of the cutout rather than at the coaming ring. The reduced area of 0.226 sq in. was used to calculate coaming-stringer stress. The influence of ring flexibility on the stringer stresses is not great in this loading case. Both rigid-ring and flexible-ring theory give good estimates of stringer stresses for the one-bay cutouts. In the case of the 130° two-bay cutout (fig. 5(d)), the maximum stringer stress is actually in closer agreement with the rigid-ring theory, but this agreement may be due in part to the neglect in the flexible-ring calculations of the influence of interrupting the ring at the center line of the cutout.

Shear Load With Cutout on Tension Side

In figures 6 and 7 are shown stresses for a loading condition of vertical shear with the cutout located on the tension side of the cylinder. The shear stresses plotted in figure 6 occur in the bay adjacent to the cutout on the root side. The experimental stresses are obtained from gages located on the center line of the bay on successive shear

panels in the circumferential direction. For the 50° and 90° cutouts (figs. 6(a) and 6(b), respectively), the theory appears to be somewhat high for the highest of these center shear stresses. For the 130° cutouts (figs. 6(c) and 6(d)), there were no gages located in the center of the shear panels where the highest shear stresses occur.

The stringer stresses shown in figure 7 occur at the coaming ring on the root side of the cutout. It is seen that the flexible-ring theory gives a satisfactory estimate of these stringer stresses for all cutout sizes plotted.

Shear Load With Cutout on Neutral Axis

Shear stresses and stringer stresses for a loading condition of vertical shear with the cutout centered on the neutral axis are shown in figures 8 and 9. As in the torsion case, the experimental shear stresses shown in figure 8 are obtained from gages located on the center line of the cutouts for the one-bay cutouts. For the 130° two-bay cutout (fig. 8(d)), the experimental shear stresses are obtained from gages on the center line of the cut bay closer to the root rather than on the cutout center line.

The greatest error in predicting the highest center shear stress for the one-bay cutouts occurs for $\beta = 90°$ (fig. 8(b)) where the theoretical value is 9 percent low. For the case of the 130° two-bay cutout (fig 8(d)), the theory predicts that the highest center shear stress in the cut bay closer to the root will occur in the shear panel adjacent to the coaming stringer whereas the highest experimental center shear stress occurs in the second panel from the coaming stringer. The largest deviation between the experimental and calculated shear stresses in these two panels, however, is only 14 percent.

The stringer stresses at the coaming ring on the tip side of the cutout are plotted in figure 9. The theory gives a satisfactory estimate of these stringer stresses for all cutout sizes plotted.

DISCUSSION

For the cases of the cylinder in torsion or under shear with the cutout on the neutral axis, the experimental data (parts (b) of tables 2 to 7 in ref. 2 and parts (c) of tables 8 to 13 in ref. 4) indicate that in each of the shear panels of the net section the shear stress is fairly constant and the center shear stress is almost always the maximum. The highest center shear stress in the net section is the maximum shear stress in the structure. Consequently, for these loading conditions (in which the stress distributions in the vicinity of the cutout resemble the

distribution in a shear-loaded sheet-stringer panel with cutout) the theory of reference 1 provides a satisfactory estimate of both the maximum stringer stress and the maximum shear stress.

For the cases of the cylinder under pure bending or shear with the cutout on the tension side, the experimental data (parts (c) of tables 2 to 6 in ref. 3 and parts (c) of tables 2 to 6 in ref. 4) indicate that a considerable variation of shear stress exists in the shear panels which have the highest shear stresses. The test results show that the maximum shear stress in these panels is not the center shear stress but the shear stress which occurs at the coaming ring. Calculation of this maximum shear stress is beyond the scope of the theory of reference 1 and requires a more refined analysis. Consequently, for these loading conditions (in which the stress distributions in the vicinity of the cutout resemble the distribution in an axially loaded sheet-stringer panel with cutout), the theory of reference 1 predicts adequately the maximum stringer stress but not the maximum shear stress.

CONCLUSIONS

Comparisons are made between a theory for calculating stresses about rectangular cutouts in circular cylinders of semimonocoque construction (NACA TN 3200) and previously published experimental data. The experimental data were obtained on a single cylinder under various loading conditions and with successively larger cutouts.

The theory provides a satisfactory estimate of stringer stresses in the neighborhood of the cutout for all the loading conditions considered in the tests. In the cases of torsion or shear with the cutout on the neutral axis, the theory provides a good approximation for the shear stresses in the center of the shear panels (center shear stresses) in the bay or bays of the net section and consequently gives the maximum shear stress in the structure. In the cases of pure bending or shear both with the cutout on the tension side, the theory also provides a good approximation for the center shear stresses except in the panels where the highest shear stresses occur. In these panels, the theoretical shear stresses are high when compared with the center shear stresses although better agreement would probably result if the theoretical stresses were compared with the true average shear stresses. For these loading conditions, however, an estimate of the maximum shear stress in the structure is beyond the scope of the theory, and comparisons for this maximum shear stress are not included in this report.

The rings in the test cylinder were stiffer than ordinarily would be used in the design of a large fuselage. The comparisons for the test cylinder, however, show that the assumption of complete rigidity of the

rings generally does not lead to a satisfactory estimate of the stresses. The flexible-ring theory agrees more closely with the test results than does the rigid-ring theory in every case except one. In the one exceptional case, that of stringer stresses for pure bending with the cutout on the tension side, the influence of ring flexibility is relatively small, and both the rigid- and flexible-ring theories give good predictions of the stringer stresses. In the flexible-ring calculations for the two-bay cutouts, neglecting the effect of interrupting the ring probably was not important.

Langley Aeronautical Laboratory,
National Advisory Committee for Aeronautics,
Langley Field, Va., August 18, 1955.

REFERENCES

1. McComb, Harvey G., Jr.: Stress Analysis of Circular Semimonocoque Cylinders With Cutouts by a Perturbation Load Technique. NACA TN 3200, 1954.

2. Schlechte, Floyd R., and Rosecrans, Richard: Experimental Stress Analysis of Stiffened Cylinders With Cutouts - Pure Torsion. NACA TN 3039, 1953.

3. Schlechte, Floyd R., and Rosecrans, Richard: Experimental Stress Analysis of Stiffened Cylinders With Cutouts - Pure Bending. NACA TN 3073, 1954.

4. Schlechte, Floyd R., and Rosecrans, Richard: Experimental Stress Analysis of Stiffened Cylinders With Cutouts - Shear Load. NACA TN 3192, 1954.

5. McComb, Harvey G., Jr., and Low, Emmet F., Jr.: Tables of Coefficients for the Analysis of Stresses About Cutouts in Circular Semimonocoque Cylinders With Flexible Rings. NACA TN 3460, 1955.

6. Biezeno, C. B., and Koch, J. J.: The Effective Width of Cylinders, Periodically Stiffened by Circular Rings. Proc. Koninklyke Nederlandsche Akademie van Wetenschappen (Netherlands), vol. XLVIII, 1945, pp. 147-165.

7. Thürliman, Bruno, Bereuter, Rudolph O., and Johnston, Bruce G.: The Effective Width of a Circular Cylindrical Shell Adjacent to a Circumferential Reinforcing Rib. Proc. First U. S. Nat. Cong. Appl. Mech. (Chicago, Ill., 1951) A.S.M.E., 1952, pp. 347-356.

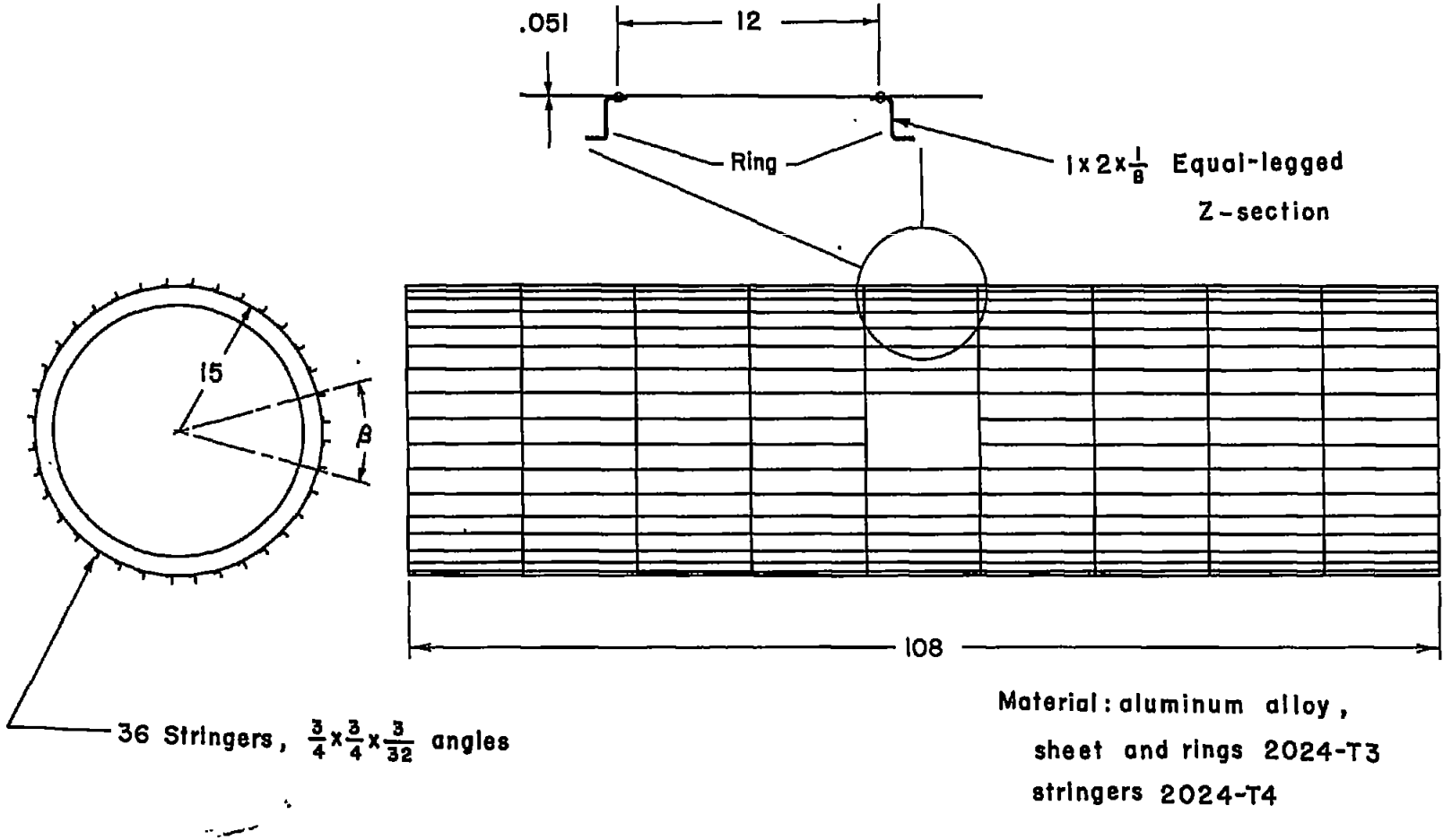

Figure 1.- Test cylinder. All dimensions are in inches.

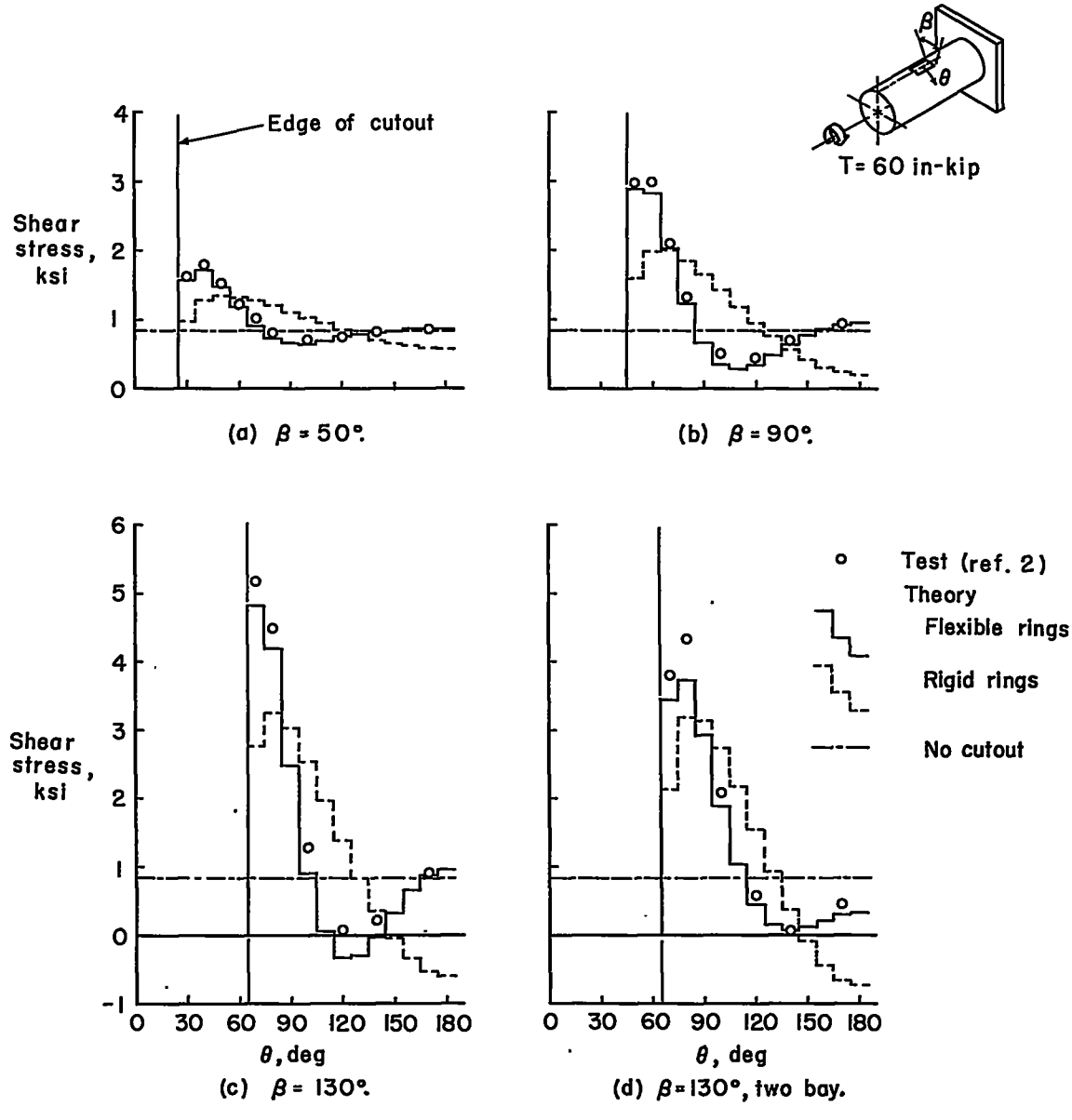

Figure 2.- Comparison between calculated shear stresses and experimental center shear stresses in net section of cylinder in torsion.

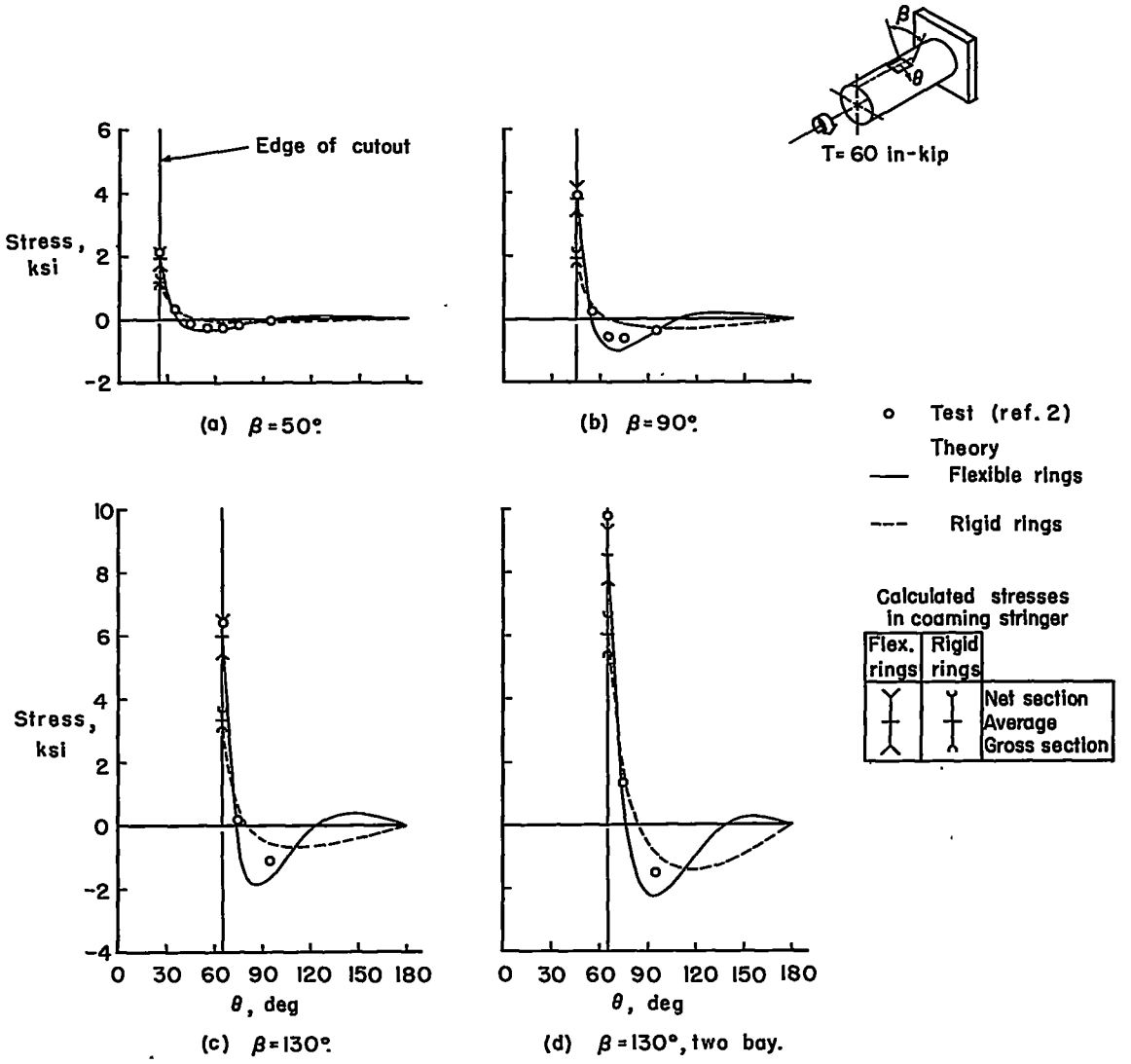

Figure 3.- Comparison between calculated and experimental stringer stresses at coaming ring in a cylinder in torsion.

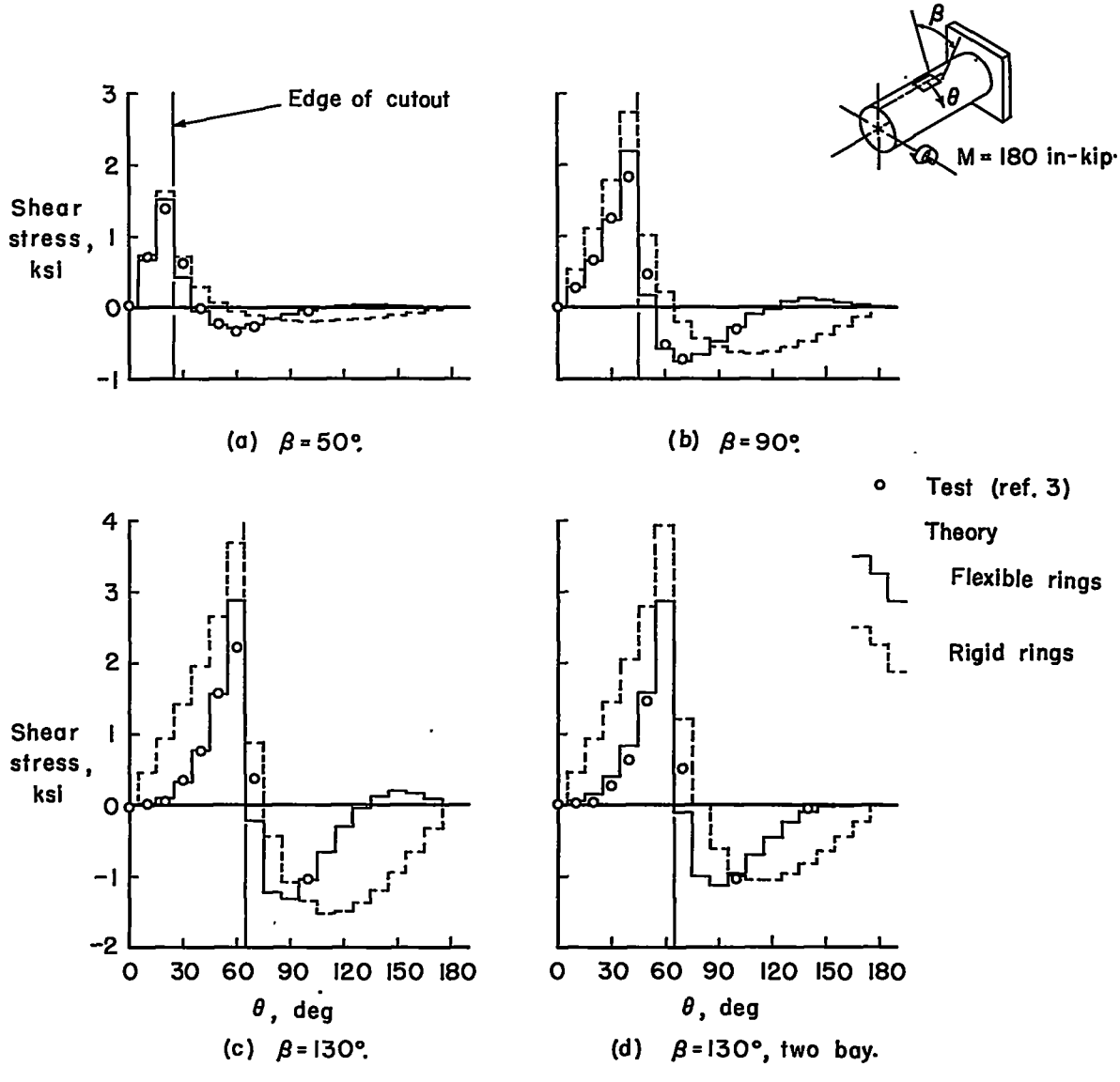

Figure 4.- Comparison between calculated shear stresses and experimental center shear stresses in bay adjacent to cutout in a cylinder in pure bending with cutout on tension side.

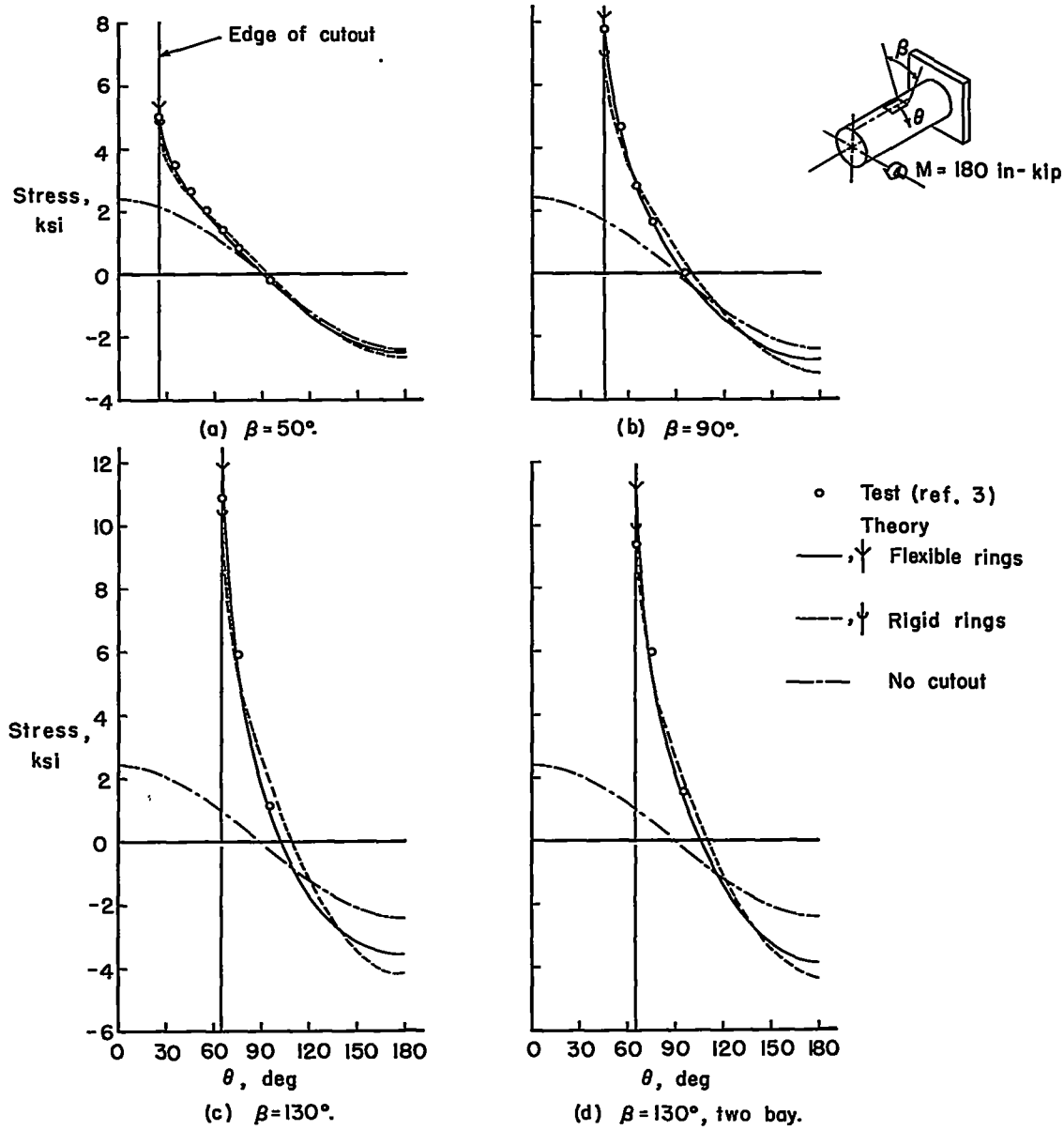

Figure 5.- Comparison between calculated and experimental stringer stresses at center line of cutout in a cylinder in pure bending with cutout on tension side.

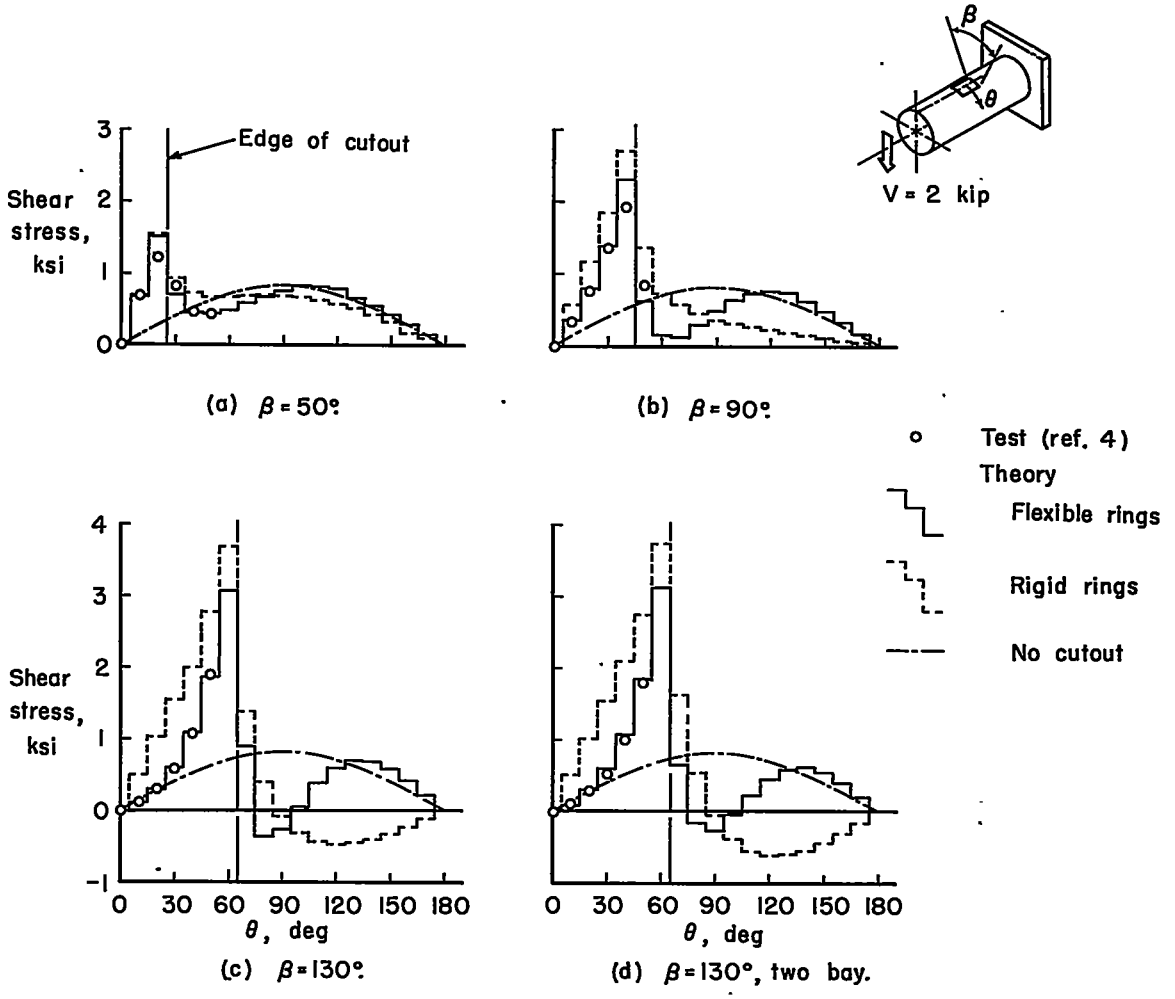

Figure 6.- Comparison between calculated shear stresses and experimental center shear stresses in bay adjacent to root side of cutout in a cylinder under shear load with cutout on tension side.

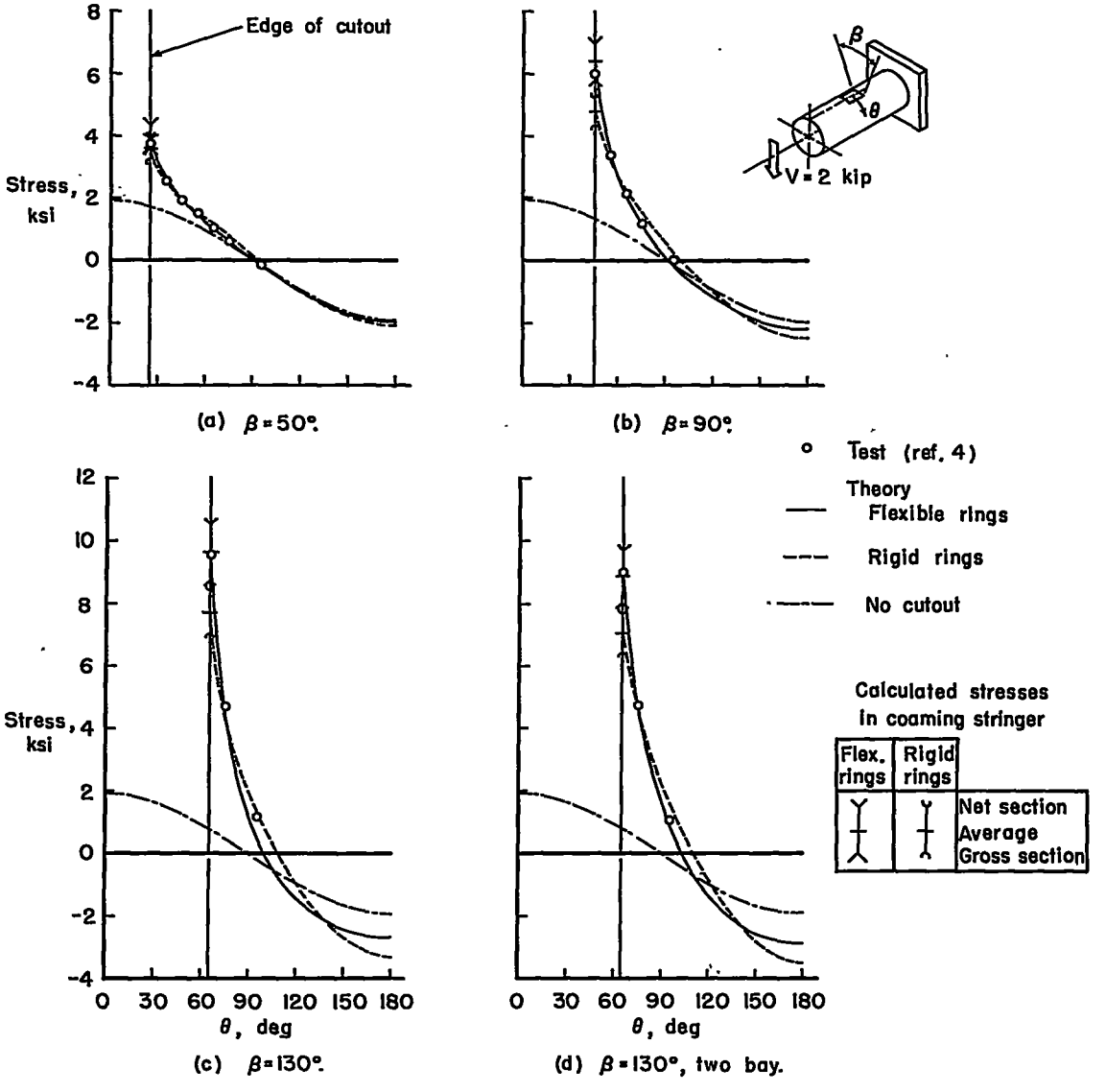

Figure 7.- Comparison between calculated and experimental stringer stresses at coaming ring on root side of cutout in a cylinder under shear load with cutout on tension side.

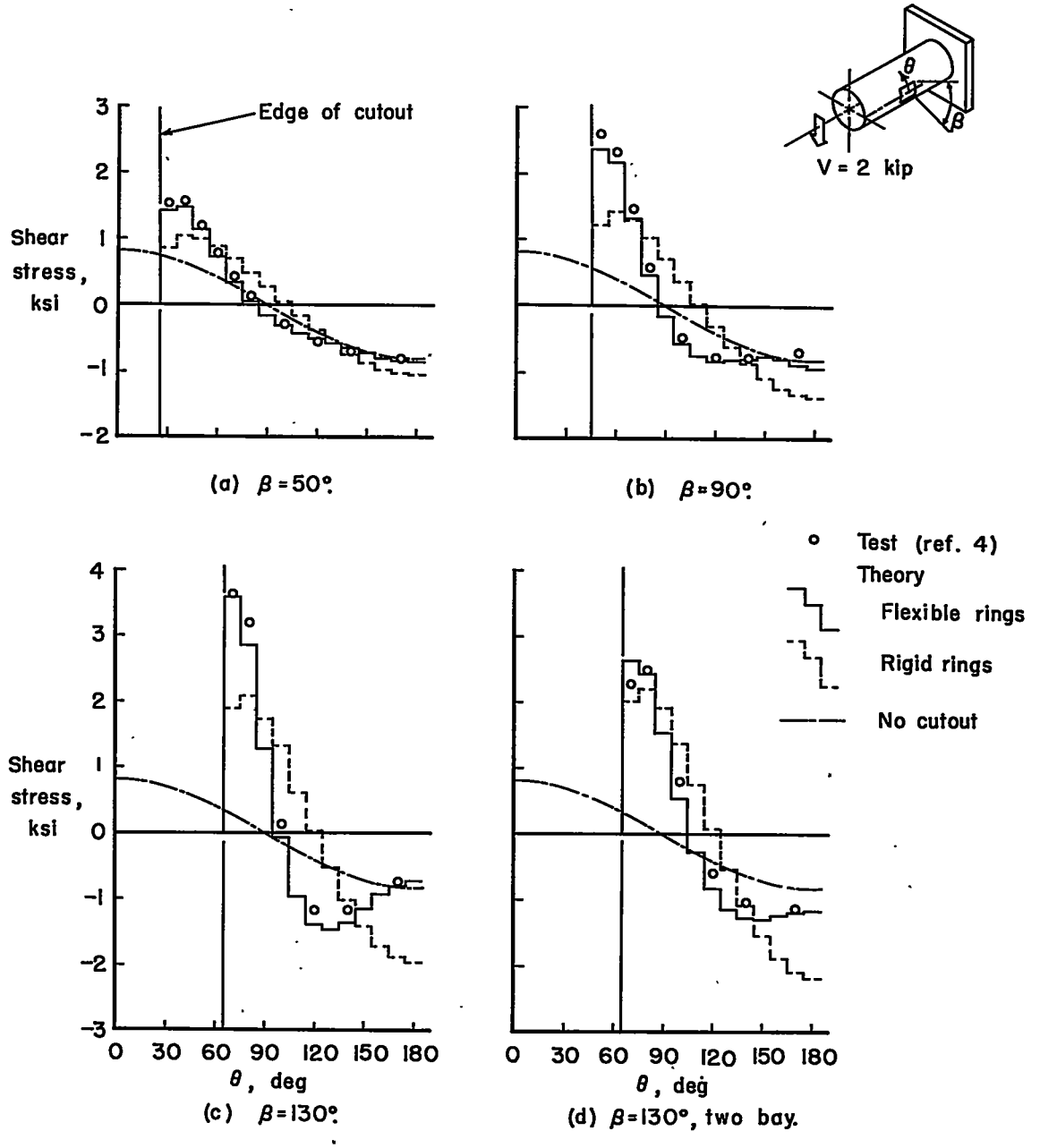

Figure 8.- Comparison between calculated shear stresses and experimental center shear stresses in net section of cylinder under shear load with cutout centered on neutral axis.

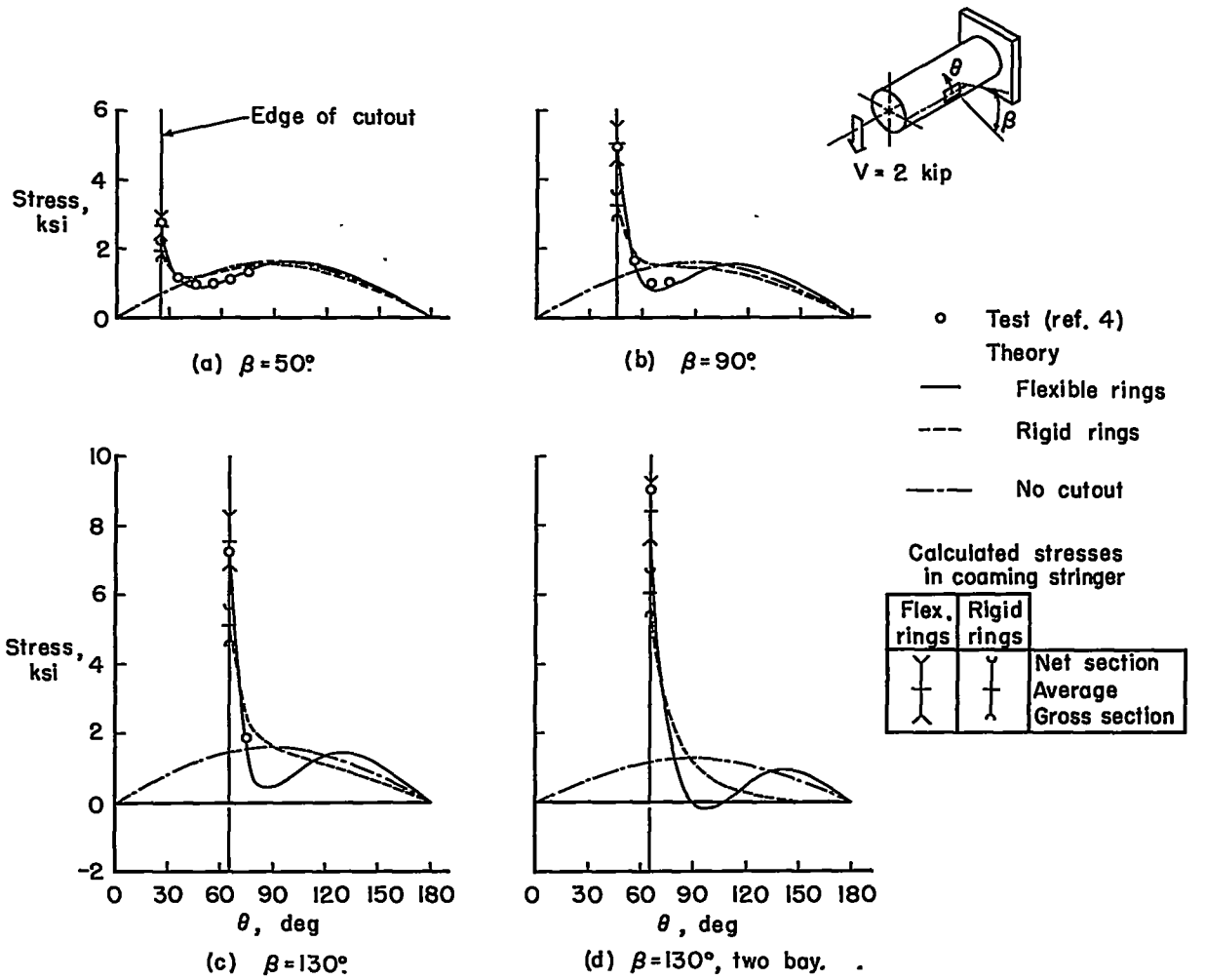

Figure 9.- Comparison between calculated and experimental stringer stresses at coaming ring on tip side of cutout in a cylinder under shear load with cutout centered on neutral axis.